Armenian Journal of Physics, 2019, vol. 12, issue 2, pp. 207-212

Anomalous Magnetic Ordering in Epitaxial $TbMnO_3$ Ultrathin Films

H.W. Lu, W.T. Wang*

Institute of Opto-Electronic Information Science and Technology, Yantai University, 264005 Yantai, P.R. China
*E-mail: whetwang@163.com

Received 06 May 2019

Abstract. Orthorhombic c-axis-oriented $TbMnO_3$ films of 24~200 nm thickness were grown epitaxially on $SrTiO_3$ (001) single crystal substrates by using pulsed laser deposition technique. The temperature (2~300 K) dependence of magnetization data were obtained on a quantum design superconducting quantum interference device. When the magnetic field was applied in the a-b plane, apart from the three magnetic ordering transitions at low temperatures (10 K, 21 K and 43 K), the magnetization evidently displayed an anomalous antiferromagnetic ordering around 156 K, which was related to the film thickness seriously. A broad transition peak at the same temperature was also observed when the applied field was along the c axis direction. The anomalies at high temperature were not observed in bulk $TbMnO_3$ materials. These results were discussed in terms of unexpected magnetic ordering of the Mn^{3+} moments induced by the interface strain between the films and the substrates.

Keywords: perovskite, thin films, magnetic properties, strain

1. Introduction

Magnetic ferroelectrics, in which both magnetic and ferroelectric orders coexist, have attracted a great deal of interest in recent years, as the simultaneous ferroic orders in the same phase can provide an additional degree of freedom in multifunctional device design [1-4]. Among these rare materials, $TbMnO_3(TMO)$, which has the orthorhombically distorted perovskite structure with lattice constants $a = 5.296, b = 5.837, c = 7.404$ Å at room temperature, is prototypical and shows unusual interplay of magnetic and electric properties. Most research focus on the antiferromagnetism and ferroelectricity properties of TMO bulk materials or single crystals at low temperature, and large magnetoelectric effects are reported [5-7].

It was suggested that the magnetic or ferroelectric polarization is accompanied by an induced lattice modulation [8]. The lattice parameter of ultrathin films is different from that of the corresponding bulk materials because of the strain induced by the mismatch between the film and the substrate. Therefore, the films and the corresponding bulk materials may exhibit different behaviors during certain physical process [9-11]. Moreover, the preparation of high-quality films is an indispensable requirement for practical applications. For this purpose, we fabricated TMO epitaxial thin films with thickness of $24 \sim 200\, nm$ by pulsed laser deposition technique to conduct a comprehensive study of their magnetic properties.

2. Experimental details

The thin films were deposited using a KeF excimer laser ($\lambda = 248\, nm, \tau = 20\, ns, 3\, Hz$ repetition rate) focused onto the high purity target of TMO ceramic. The typical energy density used was close to $2.5\, J/cm^2$, high enough to ablate the TMO. The target was mounted on a rotating holder, $40\, mm$ from the cubic $SrTiO_3(001)$ substrates $[STO(001)]$ ($a = b = c = 3.905$ Å, $0.5\, mm$ in thickness) which were maintained at $800^0 C$ during the deposition process. The experiments were carried out under vacuum at an oxygen pressure of $30\, Pa$. The thickness of the films was controlled by a film thickness monitor and samples with thickness of $24 \sim 200\, nm$

were obtained.

The crystalline structure of the deposited TMO films was investigated by X-ray diffraction (XRD) with $Cu\,K\alpha$ radiation at 1.54 Å. The surface morphology of the films was investigated by AFM (Digital Instrument Nanoscope IIIa) in contact mode with a NPS-type Si_3N_4 tip. The magnetization data were obtained using a superconducting quantum interference device (SQUID) magnetometer and corrected for demagnetization, and the measurements were carried out in a temperature range of $2 \sim 300K$ under a $200\,Oe$ applied magnetic field.

3. Results and discussion

Figure 1(a) shows typical $XRD\,\theta-2\theta$ scan profiles for the deposited TMO films ($96\,nm$) on STO (001) substrates. The diffraction peaks reveal pure $(001)-$oriented TMO reflections without impurity phases, which confirm that the films are fully epitaxial growth with $c-$orientation on STO (001) substrates. The φ scans of the (112) reflections for the TMO films and STO substrates display a clear fourfold symmetry, as shown in Fig. 1(b). Fourfold symmetry peaks are located at φ of 39^0 and 90^0 intervals for the films, and the azimuth for that of the substrate is 84^0, suggesting that the films are indeed epitaxial and well aligned with the substrate with 45^0 rotation in $a-b$ plane. By comparing Figs. 1(a) and 1(b), the epitaxial relationship between TMO and STO (001) substrate can be determined, as schematically illustrated in the inset in Fig. 1(a). The c value of the film with thickness of $96\,nm$, determined from XRD data, was about 7.443 Å, slightly larger than that of bulk TMO materials ($c_{bulk} = 7.404$ Å). The results suggested that the c axis was tense-strained because of the existing compressive strain in $a-b$ plane of the TMO crystal cell, which was originated from the lattice mismatch between the substrate and the film. The calculated c value of $200\,nm$-thick film was about 7.400 Å, almost the same with that of orthorhombic bulk TMO.

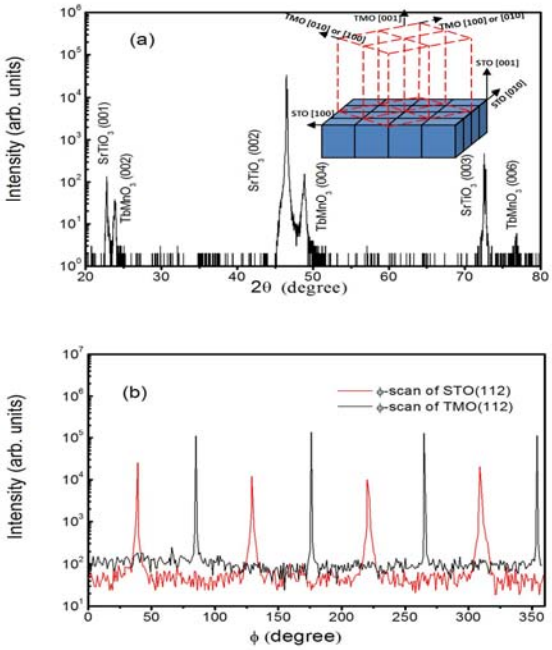

Fig. 1. (a) Typical XRD θ-2θ patterns of TMO thin films on STO(001) substrates. The inset in (a) shows the schematic model of epitaxial relationship between the films and substrates. (b) The azimuthal φ scans of the (112) peaks of TMO and STO.

Fig. 2 shows the c values of the prepared samples with different thickness. The inset shows the sketch map of TMO crystal cell. With the increasement of film thickness, the tense strain was relaxed and the length of c axis decreased and approached the value of bulk TMO materials.

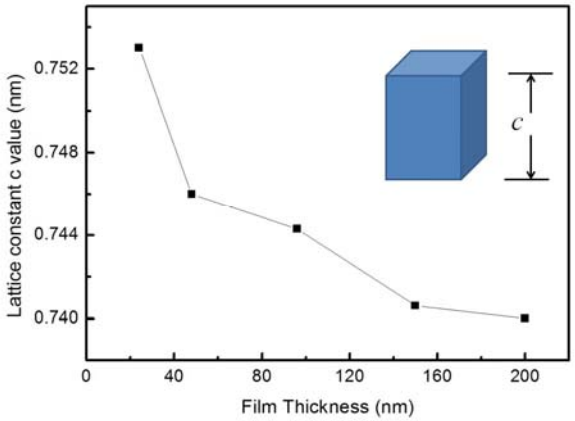

Fig. 2. Calculated c values of the prepared samples with different film thickness. The inset shows the sketch map of TMO crystal cell.

Figure 3 shows an AFM image of $1\times1\,\mu m^2$ area of a $96\,nm-$thick TMO film. The lower part of Fig. 3 gives the height profiles along the line in the image. The maximum height fluctuation is about $2.00\,nm$. The root-mean-square surface roughness is $0.533\,nm$, suggesting excellent smoothness and uniformity of the films which is important for functional device applications.

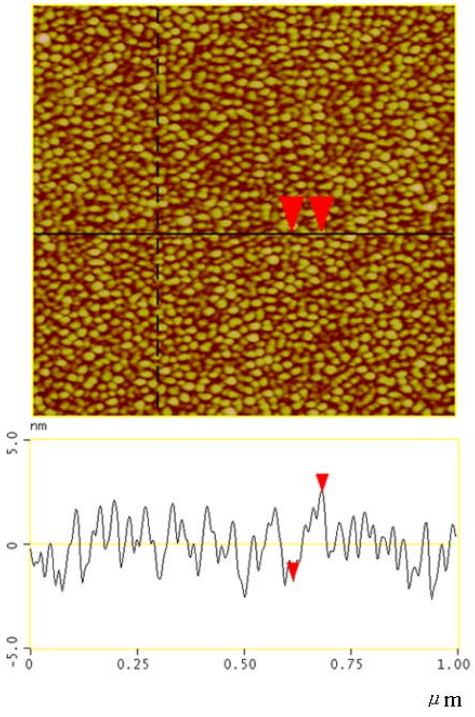

Fig. 3. AFM image of a 96nm-thick TMO film.

Figure 4 shows the magnetization versus temperature curves of a *TMO* film (96 *nm*) measured under the zero-field cooled (ZFC) and the field cooled (FC) conditions on SQUID. The applied magnetic field (200 *Oe*) is parallel to the surface of film. Both curves show anomalies near $10\,K, 21\,K$ and $43\,K$ at low temperature, which resemble those in bulk crystals and represent the magnetic ordering of the Tb^{3+} moments, the incommensurate- commensurate transition and the sine-wave ordering of the Mn^{3+} moments, respectively [2]. A new antiferromagnetic transition appeared at $156\,K$ in ZFC and FC curves, which can not be observed in thick films or bulk *TMO* materials. The ZFC temperature dependence of magnetization of *TMO* films with different thickness were shown in Fig. 5. For clarity, the data were normalized by magnetization at $10\,K(M_{10K})$. No peaks around $156\,K$ can be detected in the curves for the films with thickness more than 200nm, which is in agreement with bulk data. When thickness is less than $150\,nm$, however, the new anomalies can be seen clearly. Due to the resolution limit of our magnetometer, the anomaly of the curve (24 *nm*) is broad and inconspicuous for the feeble signal.

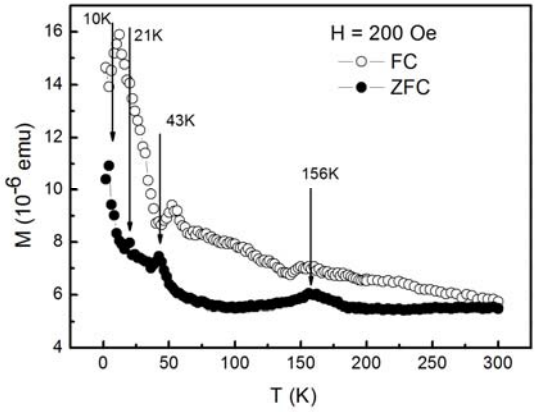

Fig. 4. ZFC and FC temperature dependence of magnetization of a TMO film (96 nm) on STO (001) substrate with an applied magnetic field of 200 Oe parallel to a-b plane.

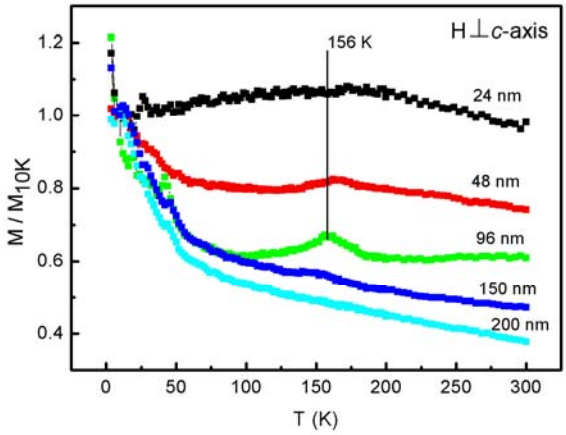

Fig. 5. ZFC magnetization normalized with M(10K) observed for TMO films measured in the a-b plane with an applied magnetic field of 200 Oe, showing the anomalies at high temperature. The thicknesses in nm are given in the plot.

The reason behind the emergence of the antiferromagnetic transition at $156K$ is not completely clear at present. It is possible that the strain in the films plays an important role in this event. Strain in the ultrathin films has been suggested to be one of the key factors that induced the difference between the bulk and film behaviors [9-11]. Besides the thermal expansion mismatch, lattice mismatch between the substrate and the film is a main origin of the internal strain [12]. As calculated from XRD data, the c value of films is different from that of bulk materials seriously when the film thickness is less than $200\,nm$, which means severe strain exists in the crystal lattice. This strain may have effects on the lattice modulation at certain epitaxial orientation and induce the change of Mn^{3+} moments. As is known, the magnetic ordering of the Mn^{3+} ions is uniaxial, and the moments are parallel to the b direction, making b axis the easy axis in the $Pb\,nm$ group symmetry setting [13]. Due to the compression strain in the $a-b$ plane of the deposited films, the Mn^{3+} moments deviate from the b axis, and incline to the c directions. The tilted Mn^{3+} moments may have orthogonal projections on b and c axes, which result in the observed magnetic ordering at high temperature.

In order to further examine this anomalous magnetization, we plot the results measured with a $200\,Oe$ field applied along the $c-$axis direction. As the c direction is not the easy axis of TMO films, the magnetization is smaller than that of b axis. As shown in Fig. 6, the ZFC curves exhibit a broad ordering transition near $156K$, which can be assigned as ordering projection of Mn^{3+} moments on c axis. When the film thickness exceed $200nm$, the strain in $a-b$ plane that originated from lattice mismatch between the substrate and the film is relaxed and the magnetic ordering of the Mn^{3+} ions is parallel to the b direction, the magnetic properties of TMO films are analogous to those of bulk materials and no anomalous transitions can be detected at high temperature.

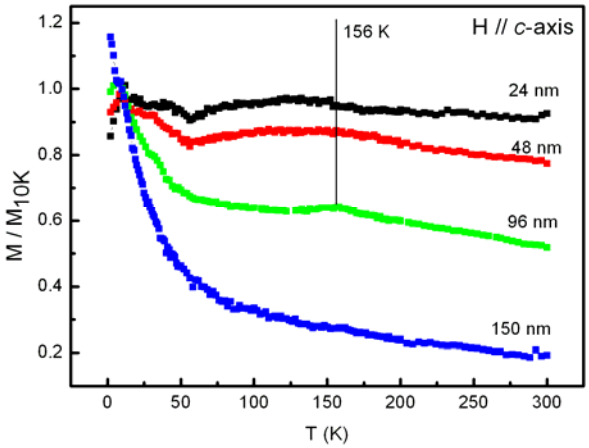

Fig. 6. ZFC magnetization normalized with M(10K) along the c axis measured at 200 Oe. The thicknesses in nm are given in the plot.

4. Conclusion

In conclusion, epitaxial TMO films with thickness $24\sim200\,nm$ were fabricated on $STO(001)$ substrates by pulsed laser deposition. The magnetic properties of the TMO films were examined on SQUID. A new transition peak was found at $\sim156K$ in ultrathin films besides the reported three anomalies of bulk TMO crystals. This interesting result may be explained possibly

by the tilted Mn^{3+} moments indued by the internal compressive strain in $a-b$ plane of the TMO crystal cell. With the increase of film thickness, the strain was relaxed and the anomalous magnetic ordering disappeared.

References

[1] W. Eerenstein, N. D. Mathur, J. F. Scott, Nature, **442** (2006) 759.
[2] T. Kimura, T. Goto, H. Shintani, K. Ishizaka, T. Arima, Y. Tokura, Nature, **426** (2003) 55.
[3] T. Lottermoser, T. Lonkai, U. Amann, D. Hohlwein, J. Ihringer, M. Fiebig, Nature, **430** (2004) 541.
[4] N. Hur, S. Park, P. A. Sharma, J. S. Ahn, S. Guha, S. W.Cheong, Nature, **429** (2004) 392.
[5] S. Mathews, R. Ramesh, T. Venkatesan, J. Benedetto, Science, **276** (1997) 238.
[6] S. Suzuki, T. Yamamoto, H. Suzuki, K. Kawaguchi, K. Takahashi, Y. Yoshisato, J. Appl. Phys., **81** (1997) 6830.
[7] C. C. Yang, M. K. Chung, W. H. Li , T. S. Chan, R. S. Liu, Y. H. Lien, C. Y. Huang, Y. Y. Chan, Y. D.Yao, J. W. Lynn, Phys. Rev. B, **74** (2006) 094409.
[8] T. Kimura, G. Lawes, T. Goto, Y. Tokura, A. P. Ramirez, Phys. Rev. B, **71** (2005) 224425.
[9] C. L. Canedy, H. Li, S. P. Alpay, L. Salamanca-Riba, A. L. Roytburd, R. Ramesh, Appl. Phys. Lett., **77** (2000) 1695.
[10] K. J. Choi, M. Biegalshi, Y. L. Li, A. Sharan, J. Schubert, R. Uecker, P. Reiche, Y. B. Chen, X. Q. Pan, V. Gopalan, L. Q. Chen, D. G. Schlom, C. B. Eom, Science, **306** (2004) 1005.
[11] J. H. Haeni, P. Irvin, W. Chang, R. Uecker, P. Reiche, Y. L. Li, S. Choudhury, W. Tian, M. E. Hawley, B. Craigo, A. K.Tagantsev, X. Q. Pan, S. K. Streiffer, L. Q. Chen, S. W. Kirchoefer, J. Levy, D. G. Schlom, Nature, **430** (2004) 758.
[12] D. Y. Wang, Y. Wang, J. Y. Dai, H. L. W. Chan, C. L. Choy, J. Electroceram., **16** (2006) 587.
[13] A. Munoz, M. T. Casais, J. A. Alonso, M. J. Martinez-Lope, J. L. Matinez, M. T. Fernandez-Diaz, Inorg. Chem., **40** (2001) 1020.